

THERMAL STABILITY OF THE U-Zr FUEL AND ITS INTERFACIAL REACTION WITH LEAD

B-S. Lee, Y. Kim, J-H. Lee, T-Y. Song
Korea Atomic Energy Research Institute
P.O. Box 105, Yuseong, Daejeon, 305-600 Korea

Abstract

The effect of heat treatment on fuel rods at 630°C and 700°C and the interfacial reaction between fuel and lead were investigated. The U-Zr metallic fuel was fabricated by mixing, pressing, sintering and extrusion. There were two kinds of phases – α -Zr precipitates and a δ -UZr₂ matrix in the U-Zr metallic fuel. After heat treatment of the extruded rod at 630°C and 700°C, the volume changes of the samples increased slightly and the density variation was negligible. Therefore, it is evident that U-Zr fuels have good thermal stability. The interface between U-55Zr fuel and Pb according to annealing time at 650°C consisted of two distinctive regions – a reaction zone in the vicinity of the surface and an initial zone in the inner area. It should be noted that the thickness of the reaction zone was 26 μm , 36 μm and 46 μm at 100 hrs, 200 hrs and 1 000 hrs, respectively. Also, the reaction zone consisted of an α -Zr layer and a Zr-depleted area.

Introduction

The blanket fuel assembly for HYPER (hybrid powder extraction reactor) contains a bundle of pins arrayed in a triangular pitch, which has a hexagonal bundle structure. The reference blanket fuel pin consists of the fuel slug of the TRU-xZr ($x = 50\text{-}60$ wt.%) alloy and is immersed in lead for thermal bonding with the cladding. The blanket fuel cladding material is ferritic-martensitic steel HT9.

Although there are lots of experimental data on the metallic alloys of U-Pu-Zr and U-Zr, they are for fuel types with a Zr fraction of less than 20 wt.%. Therefore, little data is available for the HYPER system fuel where the Zr fraction is higher than 30 wt.%. As a basic study on HYPER fuel, we fabricated U-55 wt.% Zr fuel instead of the actual TRU-Zr fuel. It appeared that no experimental data pertinent to the TRU-xZr ($x = 50\text{-}60$ wt.%) alloy existed. The U-55 wt.% Zr metallic fuel was fabricated by mixing, pressing, sintering and extrusion. This work was performed in order to investigate the microstructures and the thermal stability of the U55 wt.% Zr metallic fuel and the interfacial reaction between U-55 wt.% Zr fuel and Pb according to annealing time at 650°C.

Experimental procedure

The uranium powder was manufactured by a centrifugal atomiser and the zirconium powder (Sejong materials Co. Ltd, Korea) was prepared via the hydride-dehydride process.

The U-Zr metallic fuel was performed by mixing, pressing and sintering in optimum compaction and sintering conditions [1]. The sintered U-60 wt.% Zr was extruded by an indirect extrusion machine at 760°C and with a 13:1 extrusion ratio. Specimens of 25 mm in length were cut, vacuum-sealed in quartz tubes and annealed in a box furnace at 630°C and 700°C for up to 1 500 hrs. Sample swelling as a function of temperature and time was determined from dimensional changes. The densities of the annealed samples were calculated from the weights and dimensions. The microstructures and phase identification of the extruded rod and the annealed rod were examined by SEM and EDS. The area fraction of each phase obtained by SEM was analysed by a BMI plus ver. 4.0 (Winatech, Korea).

In order to clarify interfacial reaction between fuel and lead, a series of experiments were executed with fuel in Pb melt at 650°C for 100, 200 and 1 000 hrs. The composition of diffusion layers and the diffusion depth were analysed using SEM/EDS.

Results and discussion

Figure 1 shows uranium and zirconium particles. The mean particle sizes of the uranium and zirconium powders are 55 μm and 60 μm , respectively. Most of the uranium particles have a smooth surface and a generally near-perfect spherical shape with a few attached satellites. On the other hand, the zirconium particles fabricated by the hydride-dehydride process have an irregular morphology.

Figure 2 shows the back-scattered electron (BSE) image of the sintered sample. As can be seen in phase diagrams, the α -Zr phases are distributed in the δ phase, which is observed as a white matrix [2]. Also, small amounts of pores are found throughout the sample.

Figure 1. Photographs of the atomised (a) U powder and (b) Zr powder

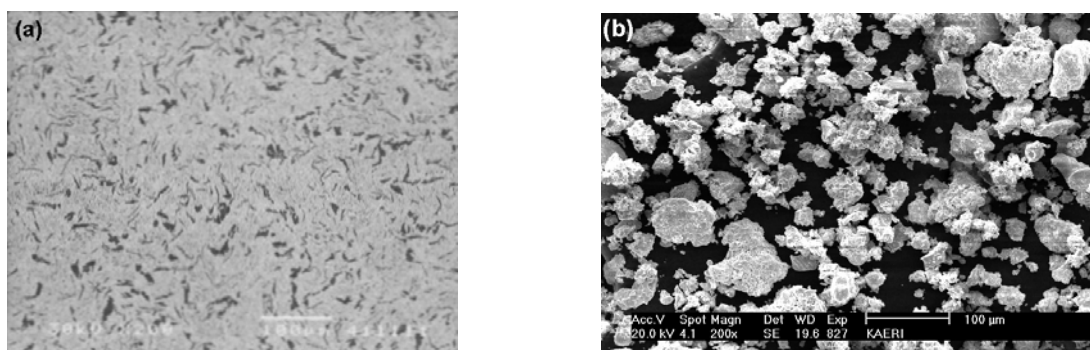
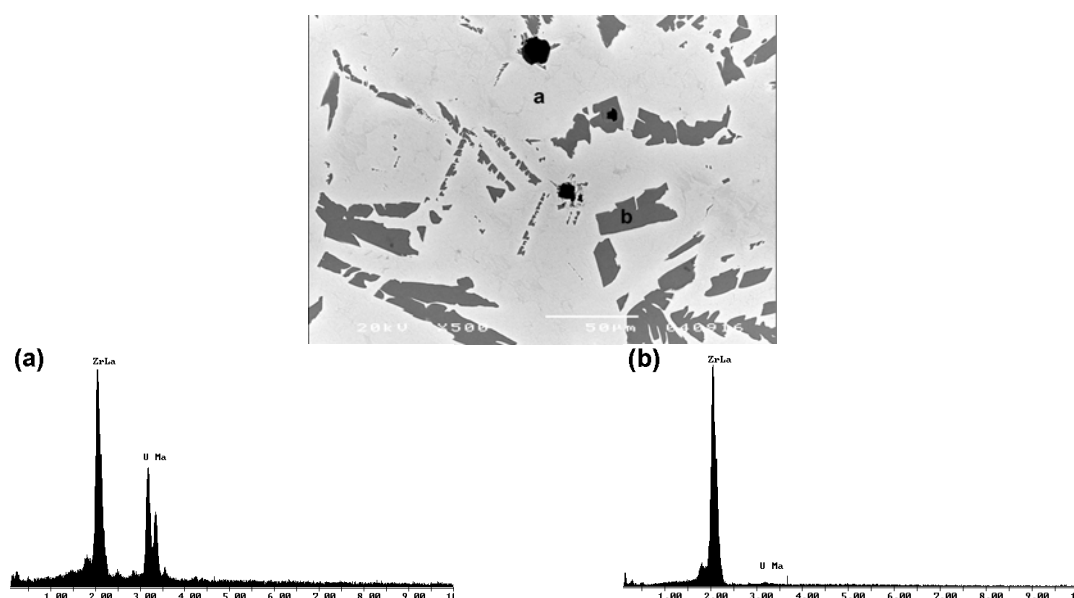


Figure 2. SEM micrograph and EDS analysis results for U-60 wt.% Zr sintered sample

(a) δ -UZr₂ matrix, (b) α -Zr phase



BSE images of the hot extruded rod are shown in Figures 3 and 4. In the sintered samples mentioned above, the α -Zr phases were also distributed (homogenously) in the white δ phase matrix and the porosity was drastically decreased because of the densification by the extrusion process. It was confirmed that the U-55 wt.% Zr alloy with a high melting point could be fabricated via a sintering process at a relatively low temperature in lieu of a conventional casting process.

Figure 5 shows the dependency of swelling behaviour and the density changes of temperature and time for the samples. The volume changes of the samples increased slightly and the density variation was negligible. Therefore, it is evident that U-55 wt.% Zr fuel has good thermal stability.

Figure 3. SEM micrographs of the extruded rod

(a) Transverse direction, (b) longitudinal direction

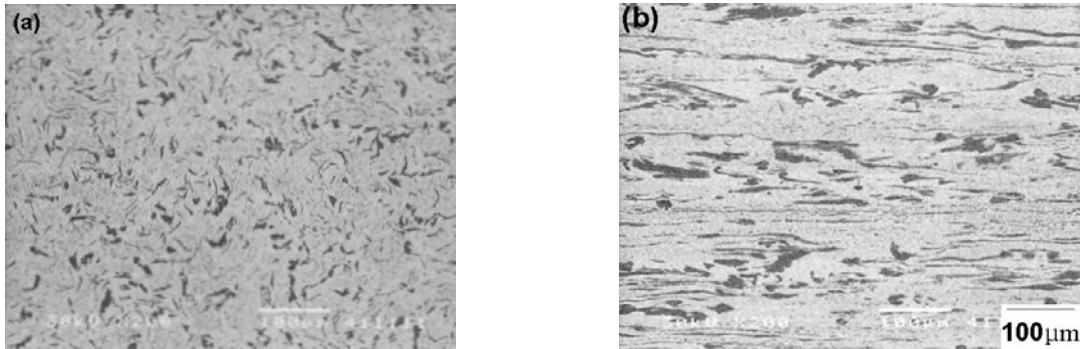


Figure 4. SEM micrograph and EDS analysis results for the extruded rod

(a) δ -UZr₂ matrix, (b) α -Zr phase

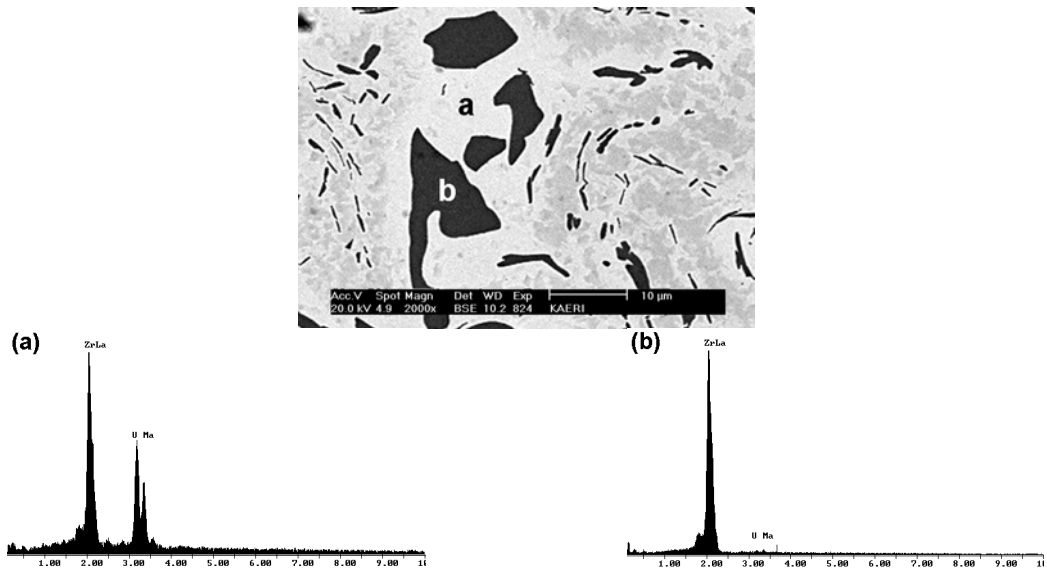


Figure 5. Volume and density changes of the extruded rod on temperature and time

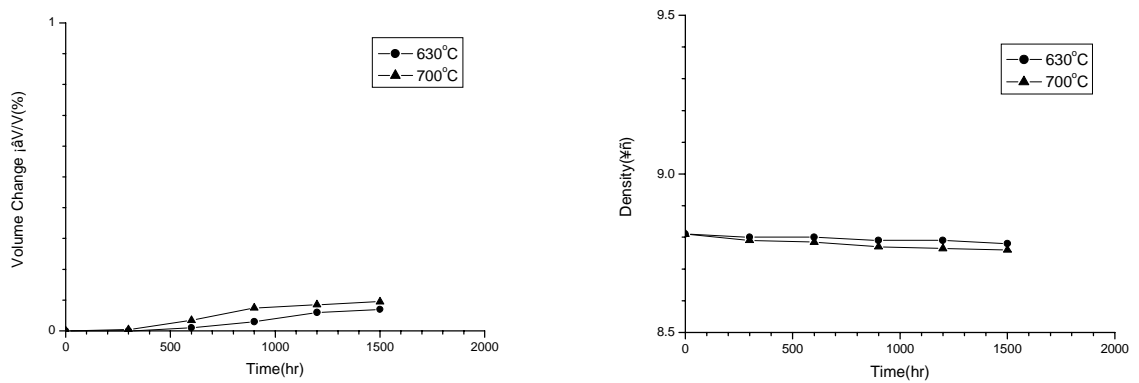


Figure 6 shows BSE images of the rod annealed at 630°C and 700°C for 600 hrs and 1 500 hrs. These figures show that as the annealing time increased, the lathed α -Zr phases began to break into pieces and grow into spherical particles. As the annealing temperature increased, spheroidising of the α -Zr phases was accelerated, with transformation to a spherical shape. We can interpret that the geometrically unstable lathed α -Zr phase transformed to the spherical phase with a lower surface area by coalescence. In addition, we think that the α -Zr and δ -UZr₂ phases dissolved and formed a solid solution at an annealing temperature above 617°C, and that the spheroidised α -Zr and δ phases appeared again during cooling.

As the annealing time increased, the hardness decreased and the decreasing rate of the hardness was much higher at 700°C than at 630°C (Figure 7). This is attributed to the increase of the area fraction of the δ phase and the decrease of the area fraction of the relatively hard α -Zr phase as the annealing temperature and time increased.

Figure 8 shows the area fraction of the α -Zr phase according to the annealing time at 630°C and 700°C. In the case of 630°C of annealing time, the area fraction of the α -Zr phase gradually decreased as the annealing time increased, whereas the area fraction of the α -Zr phase sharply decreased at the early stage of annealing time and then the decreasing rate declined at 700°C. This phenomenon agreed with the results on hardness values vis-à-vis annealing time as shown in Figure 7. When the U-55 wt.% Zr alloy is annealed at above 617°C, which is the unstable region of α -Zr phase, the alloy is diffused into the uranium matrix and finally forms δ phase at a lower temperature. Hence, it can be interpreted that the drastic decrease of area fraction of the α -Zr phase at the early stage of annealing time was due to the higher concentration gradient of Zr, which is the driving force of Zr diffusion.

Figure 6. SEM micrographs of the U-55 wt.% Zr fuel annealed at 630°C and 700°C for 600 hrs and 1 500 hrs

(a)(b) 630 °C, (c)(d) 700 °C, (a)(c) 600 hrs, (b)(d) 1 500 hrs

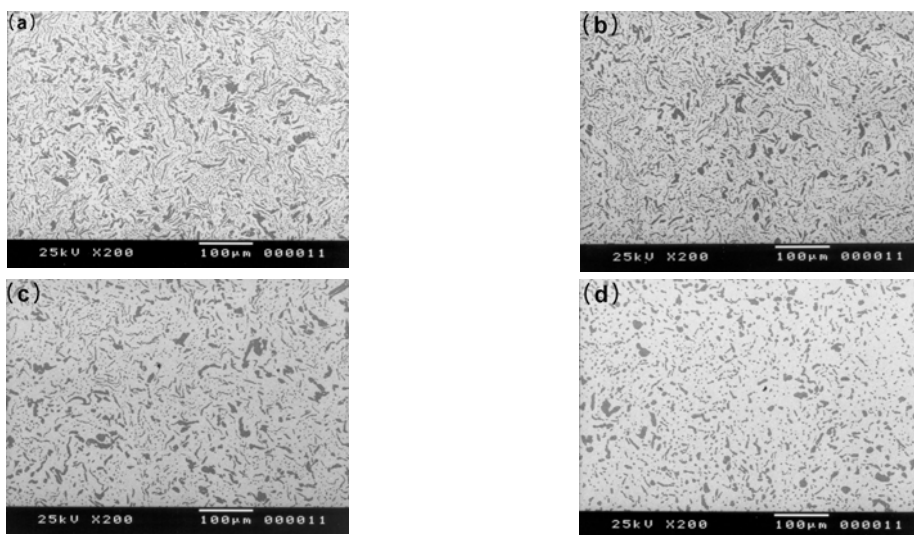


Figure 7. Variation of room temperature hardness of rods after annealing at 630°C and 700°C

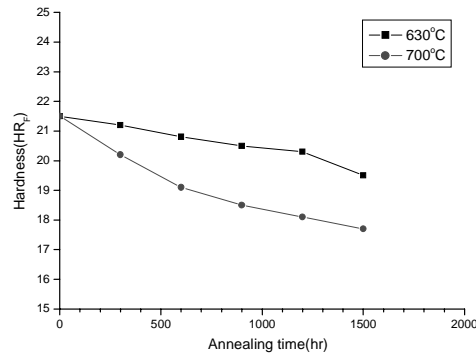


Figure 8. Variation of area fraction of α -Zr phase with annealing times at 630°C and 700°C

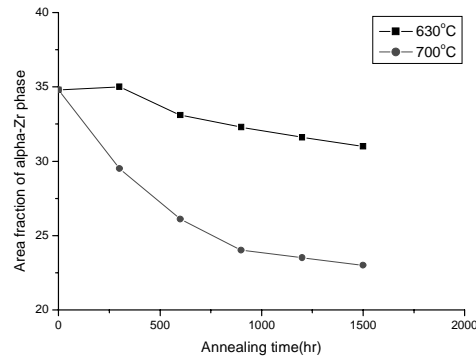


Figure 9 shows EDS line profile results on the interface between U-55Zr and Pb according to annealing time at 650°C. The microstructures of each sample consisted of two distinctive regions – a reaction zone in the vicinity of the surface and an initial zone in the inner area. It should be noted that the thickness of the reaction zone was 26 μm , 36 μm and 46 μm at 100 hrs, 200 hrs and 1 000 hrs, respectively, as the annealing time increased. The reaction zone also consisted of two regions – an α -Zr layer and a Zr-depleted area. The α -Zr layer may be formed by a diffusivity difference between U and Zr atoms (i.e. Zr atom diffuses into the Pb melt during annealing while U is relatively intact due to lower diffusivity). The TRU in the metallic fuel is reported to react with stainless, as a cladding material then forms eutectic at a low temperature. Thus, it is anticipated that the α -Zr layer should effectively act as a reaction barrier with the cladding material.

In order to closely investigate the reaction layer, EDS analysis was performed as shown in Figure 10. The analysis shows that a negligible amount of Pb is present in the very outer layer of the reaction zone with Zr-rich phase (region A). And the α -Zr phase forms a thick layer of $\sim 10 \mu\text{m}$ underneath the surface (region B). Region C consists of U-rich phase and Zr formed by the decomposition of δ phase. As the annealing time increased, the thickness of the reaction layer from A to C increased to the direction of as-extruded area, region D.

Figure 9. Line profiles of interface of U-55Zr fuel with Pb bonding according to annealing time at 650°C

(a) 100 hrs, (b) 200 hrs, (c) 1 000 hrs

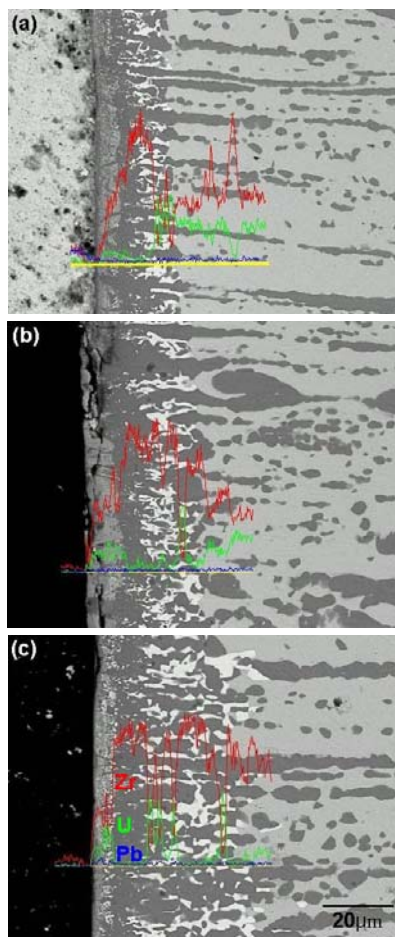
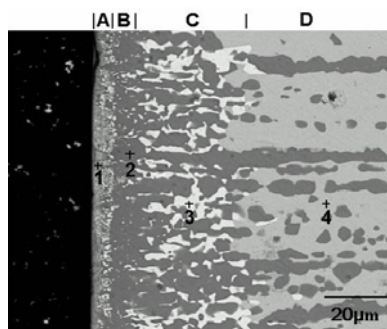


Figure 10. SEM/EDS results of U-55Zr with Pb bonding for 1 000 hrs at 650°C



Mark	Pb	U	Zr
1	0.76	19.11	80.13
2		0.37	99.63
3		95.11	4.89
4		31.82	68.18

Figures in at. %.

Conclusions

- The α -Zr phases were distributed in the white δ -UZr₂ phase matrix and the porosity was drastically decreased due to densification from the extrusion process.
- The volume changes of the samples increased slightly and the density variation was negligible. Therefore, it is evident that U-55 wt.% Zr fuel has good thermal stability.
- As annealing time increased, hardness decreased and the decreasing rate of hardness was much higher at 700°C than 630°C. This is attributed to the increase of area fraction of δ phase and the decrease of area fraction of relatively hard α -Zr phase as annealing temperature and time increased.
- The interface between U-55Zr fuel and Pb at annealing time and 650°C consisted of a reaction zone and an initial zone in the inner area. The reaction zone consisted of a α -Zr layer and a Zr-depleted area with thicknesses of 26 μm (100 hrs), 36 μm (200 hrs), 46 μm (1 000 hrs).

REFERENCES

- [1] Cho, H.S., *et al.*, *Proceedings of the Korean Nuclear Society Spring Meeting*, Jeju, Korea, May 2001.
- [2] *Phase Transformation in Materials*, 2nd Ed., D.A. Porter, K.E. Easterling (1992).

SUMMARIES OF TECHNICAL SESSIONS

Chairs: R. Sheffield, B-H. Choi

The summaries contained in this section reflect the views of the respective Chairperson(s) and do not necessarily reflect the views of the technical session group members.

TABLE OF CONTENTS

Foreword	3
Executive Summary.....	11
Welcome.....	15
<i>D-S. Yoon</i> Congratulatory Address	17
<i>I-S. Chang</i> Welcome Address	19
<i>G.H. Marcus</i> OECD Welcome	21
GENERAL SESSION: ACCELERATOR PROGRAMMES AND APPLICATIONS.....	23
<i>CHAIRS: B-H. CHOI, R. SHEFFIELD</i>	
<i>T. Mukaiyama</i> Background/Perspective.....	25
<i>M. Salvatores</i> Accelerator-driven Systems in Advanced Fuel Cycles	27
<i>S. Noguchi</i> Present Status of the J-PARC Accelerator Complex	37
<i>H. Takano</i> R&D of ADS in Japan.....	45
<i>R.W. Garnett, A.J. Jason</i> Los Alamos Perspective on High-intensity Accelerators.....	57
<i>J-M. Lagniel</i> French Accelerator Research for ADS Developments.....	69
<i>T-Y. Song, J-E. Cha, C-H. Cho, C-H. Cho, Y. Kim, B-O. Lee, B-S. Lee, W-S. Park, M-J. Shin</i> Hybrid Power Extraction Reactor (HYPER) Project	81

<i>V.P. Bhatnagar, S. Casalta, M. Hugon</i> Research and Development on Accelerator-driven Systems in the EURATOM 5 th and 6 th Framework Programmes.....	89
<i>S. Monti, L. Picardi, C. Rubbia, M. Salvatores, F. Troiani</i> Status of the TRADE Experiment.....	101
<i>P. D'hondt, B. Carlucci</i> The European Project PDS-XADS “Preliminary Design Studies of an Experimental Accelerator-driven System”.....	113
<i>F. Groeschel, A. Cadiou, C. Fazio, T. Kirchner, G. Laffont, K. Thomsen</i> Status of the MEGAPIE Project.....	125
<i>P. Pierini, L. Burgazzi</i> ADS Accelerator Reliability Activities in Europe	137
<i>W. Gudowski</i> ADS Neutronics	149
<i>P. Coddington</i> ADS Safety	151
<i>Y. Cho</i> Technological Aspects and Challenges for High-power Proton Accelerator-driven System Application.....	153
TECHNICAL SESSION I: ACCELERATOR RELIABILITY.....	163
<i>CHAIRS: A. MUELLER, P. PIERINI</i>	
<i>D. Vandeplasseche, Y. Jongen (for the PDS-XADS Working Package 3 Collaboration)</i> The PDS-XADS Reference Accelerator	165
<i>N. Ouchi, N. Akaoka, H. Asano, E. Chishiro, Y. Namekawa, H. Suzuki, T. Ueno, S. Noguchi, E. Kako, N. Ohuchi, K. Saito, T. Shishido, K. Tsuchiya, K. Ohkubo, M. Matsuoka, K. Sennyu, T. Murai, T. Ohtani, C. Tsukishima</i> Development of a Superconducting Proton Linac for ADS.....	175
<i>C. Miélot</i> Spoke Cavities: An Asset for the High Reliability of a Superconducting Accelerator; Studies and Test Results of a $\beta = 0.35$, Two-gap Prototype and its Power Coupler at IPN Orsay	185
<i>X.L. Guan, S.N. Fu, B.C. Cui, H.F. Ouyang, Z.H. Zhang, W.W. Xu, T.G. Xu</i> Chinese Status of HPPA Development	195

<i>J.L. Biarrotte, M. Novati, P. Pierini, H. Safa, D. Uriot</i> Beam Dynamics Studies for the Fault Tolerance Assessment of the PDS-XADS Linac	203
<i>P.A. Schmelzbach</i> High-energy Beat Transport Lines and Delivery System for Intense Proton Beams	215
<i>M. Tanigaki, K. Mishima, S. Shiroya, Y. Ishi, S. Fukumoto, S. Machida, Y. Mori, M. Inoue</i> Construction of a FFAG Complex for ADS Research in KURRI	217
<i>G. Ciavola, L. Celona, S. Gammino, L. Andò, M. Presti, A. Galatà, F. Chines, S. Passarello, XZh. Zhang, M. Winkler, R. Gobin, R. Ferdinand, J. Sherman</i> Improvement of Reliability of the TRASCO Intense Proton Source (TRIPS) at INFN-LNS	223
<i>R.W. Garnett, F.L. Krawczyk, G.H. Neuschaefer</i> An Improved Superconducting ADS Driver Linac Design.....	235
<i>A.P. Durkin, I.V. Shumakov, S.V. Vinogradov</i> Methods and Codes for Estimation of Tolerance in Reliable Radiation-free High-power Linac	245
<i>S. Henderson</i> Status of the Spallation Neutron Source Accelerator Complex	257
TECHNICAL SESSION II: TARGET, WINDOW AND COOLANT TECHNOLOGY.....	265
CHAIRS: X. CHENG, T-Y. SONG	
<i>Y. Kurata, K. Kikuchi, S. Saito, K. Kamata, T. Kitano, H. Oigawa</i> Research and Development on Lead-bismuth Technology for Accelerator-driven Transmutation System at JAERI	267
<i>P. Michelato, E. Bari, E. Cavaliere, L. Monaco, D. Sertore, A. Bonucci, R. Giannantonio, L. Cinotti, P. Turroni</i> Vacuum Gas Dynamics Investigation and Experimental Results on the TRASCO ADS Windowless Interface	279
<i>J-E. Cha, C-H. Cho, T-Y. Song</i> Corrosion Tests in the Static Condition and Installation of Corrosion Loop at KAERI for Lead-bismuth Eutectic	291
<i>P. Schuurmans, P. Kupschus, A. Verstrepen, J. Cools, H. Ait Abderrahim</i> The Vacuum Interface Compatibility Experiment (VICE) Supporting the MYRRHA Windowless Target Design	301

<i>C-H. Cho, Y. Kim, T-Y. Song</i> Introduction of a Dual Injection Tube for the Design of a 20 MW Lead-bismuth Target System.....	313
<i>H. Oigawa, K. Tsujimoto, K. Kikuchi, Y. Kurata, T. Sasa, M. Umeno, K. Nishihara, S. Saito, M. Mizumoto, H. Takano, K. Nakai, A. Iwata</i> Design Study Around Beam Window of ADS.....	325
<i>S. Fan, W. Luo, F. Yan, H. Zhang, Z. Zhao</i> Primary Isotopic Yields for MSDM Calculations of Spallation Reactions on ²⁸⁰ Pb with Proton Energy of 1 GeV.....	335
<i>N. Tak, H-J. Neitzel, X. Cheng</i> CFD Analysis on the Active Part of Window Target Unit for LBE-cooled XADS.....	343
<i>T. Sawada, M. Orito, H. Kobayashi, T. Sasa, V. Artisyuk</i> Optimisation of a Code to Improve Spallation Yield Predictions in an ADS Target System.....	355
TECHNICAL SESSION III: SUBCRITICAL SYSTEM DESIGN AND ADS SIMULATIONS.....	363
<i>CHAIRS: W. GUDOWSKI, H. OIGAWA</i>	
<i>T. Misawa, H. Unesaki, C.H. Pyeon, C. Ichihara, S. Shiroya</i> Research on the Accelerator-driven Subcritical Reactor at the Kyoto University Critical Assembly (KUCA) with an FFAG Proton Accelerator.....	365
<i>K. Nishihara, K. Tsujimoto, H. Oigawa</i> Improvement of Burn-up Swing for an Accelerator-driven System	373
<i>S. Monti, L. Picardi, C. Ronsivalle, C. Rubbia, F. Troiani</i> Status of the Conceptual Design of an Accelerator and Beam Transport Line for Trade.....	383
<i>A.M. Degtyarev, A.K. Kalugin, L.I. Ponomarev</i> Estimation of some Characteristics of the Cascade Subcritical Molten Salt Reactor (CSMSR).....	393
<i>F. Roelofs, E. Komen, K. Van Tichelen, P. Kupschus, H. Ait Abderrahim</i> CFD Analysis of the Heavy Liquid Metal Flow Field in the MYRRHA Pool.....	401
<i>A. D'Angelo, B. Arien, V. Sobolev, G. Van den Eynde, H. Ait Abderrahim, F. Gabrielli</i> Results of the Second Phase of Calculations Relevant to the WPPT Benchmark on Beam Interruptions	411

TECHNICAL SESSION IV: SAFETY AND CONTROL OF ADS 423

CHAIRS: J-M. LAGNIEL, P. CODDINGTON

*P. Coddington, K. Mikityuk, M. Schikorr, W. Maschek,
R. Sehgal, J. Champigny, L. Mansani, P. Meloni, H. Wider*
Safety Analysis of the EU PDS-XADS Designs..... 425

*X-N. Chen, T. Suzuki, A. Rineiski, C. Matzerath-Boccaccini,
E. Wiegner, W. Maschek*
Comparative Transient Analyses of Accelerator-driven Systems
with Mixed Oxide and Advanced Fertile-free Fuels 439

P. Coddington, K. Mikityuk, R. Chawla
Comparative Transient Analysis of Pb/Bi
and Gas-cooled XADS Concepts 453

B.R. Sehgal, W.M. Ma, A. Karbojian
Thermal-hydraulic Experiments on the TALL LBE Test Facility 465

K. Nishihara, H. Oigawa
Analysis of Lead-bismuth Eutectic Flowing into Beam Duct..... 477

P.M. Bokov, D. Ridikas, I.S. Slessarev
On the Supplementary Feedback Effect Specific
for Accelerator-coupled Systems (ACS)..... 485

W. Haeck, H. Ait Abderrahim, C. Wagemans
 K_{eff} and K_s Burn-up Swing Compensation in MYRRHA 495

TECHNICAL SESSION V: ADS EXPERIMENTS AND TEST FACILITIES 505

CHAIRS: P. D'HONDT, V. BHATNAGAR

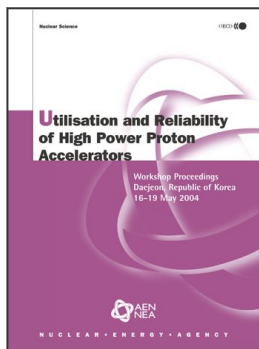
*H. Oigawa, T. Sasa, K. Kikuchi, K. Nishihara, Y. Kurata, M. Umeno,
K. Tsujimoto, S. Saito, M. Futakawa, M. Mizumoto, H. Takano*
Concept of Transmutation Experimental Facility 507

M. Hron, M. Mikisek, I. Peka, P. Hosnedl
Experimental Verification of Selected Transmutation Technology and Materials
for Basic Components of a Demonstration Transmuter with Liquid Fuel
Based on Molten Fluorides (Development of New Technologies for
Nuclear Incineration of PWR Spent Fuel in the Czech Republic) 519

Y. Kim, T-Y. Song
Application of the HYPER System to the DUPIC Fuel Cycle..... 529

M. Plaschy, S. Pelloni, P. Coddington, R. Chawla, G. Rimpault, F. Mellier
Numerical Comparisons Between Neutronic Characteristics of MUSE4
Configurations and XADS-type Models 539

<i>B-S. Lee, Y. Kim, J-H. Lee, T-Y. Song</i> Thermal Stability of the U-Zr Fuel and its Interfacial Reaction with Lead	549
SUMMARIES OF TECHNICAL SESSIONS	557
<i>CHAIRS: R. SHEFFIELD, B-H. CHOI</i>	
<i>Chairs: A.C. Mueller, P. Pierini</i> Summary of Technical Session I: Accelerator Reliability	559
<i>Chairs: X. Cheng, T-Y. Song</i> Summary of Technical Session II: Target, Window and Coolant Technology	565
<i>Chairs: W. Gudowski, H. Oigawa</i> Summary of Technical Session III: Subcritical System Design and ADS Simulations.....	571
<i>Chairs: J-M. Lagniel, P. Coddington</i> Summary of Technical Session IV: Safety and Control of ADS	575
<i>Chairs: P. D'hondt, V. Bhatagnar</i> Summary of Technical Session V: ADS Experiments and Test Facilities.....	577
SUMMARIES OF WORKING GROUP DISCUSSION SESSIONS	581
<i>CHAIRS: R. SHEFFIELD, B-H. CHOI</i>	
<i>Chair: P.K. Sigg</i> Summary of Working Group Discussion on Accelerators.....	583
<i>Chair: W. Gudowski</i> Summary of Working Group Discussion on Subcritical Systems and Interface Engineering	587
<i>Chair: P. Coddington</i> Summary of Working Group Discussion on Safety and Control of ADS.....	591
<i>Annex 1: List of workshop organisers</i>	<i>595</i>
<i>Annex 2: List of participants.....</i>	<i>597</i>



From:

Utilisation and Reliability of High Power Proton Accelerators

Workshop Proceedings, Daejeon, Republic of Korea, 16-19 May 2004

Access the complete publication at:

<https://doi.org/10.1787/9789264013810-en>

Please cite this chapter as:

Lee, B.-S., *et al.* (2006), "Thermal Stability of the U-Zr Fuel and its Interfacial Reaction with Lead", in OECD/ Nuclear Energy Agency, *Utilisation and Reliability of High Power Proton Accelerators: Workshop Proceedings, Daejeon, Republic of Korea, 16-19 May 2004*, OECD Publishing, Paris.

DOI: <https://doi.org/10.1787/9789264013810-55-en>

This document, as well as any data and map included herein, are without prejudice to the status of or sovereignty over any territory, to the delimitation of international frontiers and boundaries and to the name of any territory, city or area. Extracts from publications may be subject to additional disclaimers, which are set out in the complete version of the publication, available at the link provided.

The use of this work, whether digital or print, is governed by the Terms and Conditions to be found at <http://www.oecd.org/termsandconditions>.